Monoplanar Camera Calibration

Iterative Multi-Step Approach

Jorge Batista, Jorge Dias, Helder Araújo, A. Traça de Almeida
Institute of Systems and Robotics
Department of Electrical Engineering - University of Coimbra
Largo Marquês de Pombal-3000 COIMBRA PORTUGAL
Email : jorbat@uc.pt

Abstract

A new method for robotics camera calibration based on a linear computation and using a coplanar group of calibration points is presented in this paper. This new method suppresses the constraint presented by the RAC calibration model of having an incidence angle between the optical axis and the calibration plane of at least 30 degrees. The parameters are obtained based on a multi-step calculation, and the accuracy of the parameters is strongly increased when used on a iterative calibration. Experimental and simulated analyses results are presented. A comparative analysis between this new method and the RAC method is presented.

1. Introduction

From the mathematical point of view, an image is a projection of a three dimensional space onto a two dimensional space. Geometric camera calibration is the process of determining the 2D-3D mapping between the camera and the world coordinate system.

Most of the camera calibration techniques are polarized between approaches closely related to the classical Photogrammetry approach where accuracy is emphasized, and the approaches geared for automation and robotics, where speed and autonomy are emphasized.

The RAC calibration model presented by R. Tsai [9][10] was the first camera calibration model that included radial geometric distortion, uses linear computation methods and a coplanar group of points for calibration. However, the RAC model requires that the angle of incidence between the optical axis and the calibration plane be of at least 30 degrees.

The new method for robotics camera calibration presented in this paper, uses a coplanar group of points, suppressing the constraint of having an incidence angle of at least 30 degrees required by the RAC model. The computation of the calibration parameters is linear, and can be decomposed into four steps: (1) rotation matrix calculation, (2) translation over X and Y axis and horizontal uncertainty scale factor S_X, (3) effective focal length, radial distortion coefficient and translation over Z, and (4) image scale factors, image center coordinates and ortoghonality deviation of the image referencial axis.

The major contribution for this new method relates with the computation of the rotation matrix. The basic principle that leads to the rotation matrix calculation was first presented by Haralick [8] and is based on the fact that there is sufficient information on the 2D perspective projection of a rectangle of unknown size in 3D space to determine the camera look angle parameters. With the knowledge of the rotation matrix, the translation vector and some of the intrinsic parameters can be

obtained using the relationship that defines the same ratio between the image (u'',v'') and camera (x_C,y_C) coordinates to obtain the translation in X and Y axis and the horizontal uncertainty scale factor, followed by the relationship used in the RAC model to obtain the Z component of the translation vector, and the distortion coefficient $\mathbf{k_1}$. The procedure that we use for the computation of the effective focal length $\boldsymbol{f}$ is different from the one presented by Tsai. In this new method we assume an initial value for the focal length, and we update this value using the Gauss lens law and the perspective transformation determined on the plane that includes the line of sight and the optical axis of the lens.

With the knowledge of these parameters (**Rot**,**Trans**,$\boldsymbol{f}$,$\mathbf{k_1}$), the image scale factors, image center coordinates and ortoghonality deviation can be obtained by using the perspective transformation and the transformation between real image coordinates to pixels image coordinates.

2. Camera Model

In the following, the underlying camera model (fig. 1) is described briefly, making note of the parameters that need to be calculated through the calibration procedure.

The overall transformation from the 3D object coordinates $P_{(x,y,z)}$ to the computer image frame buffer coordinates $p(u_f,v_f)$ can be decomposed into the following steps:

1) Rigid body transformation from the object world coordinates to the 3D camera coordinates system

$$\begin{bmatrix} x_c & y_c & z_c \end{bmatrix}^T = \mathbf{Rot} \cdot \begin{bmatrix} x & y & z \end{bmatrix}^T + \mathbf{Trans} \tag{2.1}$$

where **Rot** is the rotation matrix and **Trans** the translation vector.

2) Projection from 3D camera coordinate $P(x_C,y_C,z_C)$ to the ideal image coordinate (u'',v''), using perspective projection with pin-hole camera geometry

$$u'' = \boldsymbol{f} \cdot \frac{x_c}{z_c} \qquad\qquad v'' = \boldsymbol{f} \cdot \frac{y_c}{z_c} \tag{2.2}$$

3) Transformation between ideal perspective projection coordinates and real (distorted) perspective projection coordinates, using just one distortion coefficient

$$u_d'' = \frac{2 \cdot u''}{D} \qquad\qquad v_d'' = \frac{2 \cdot v''}{D} \tag{2.3}$$

where $D=1+(1-4\cdot\mathbf{k_1}\cdot R_{ideal}^2)^{1/2}$, being $R_{ideal}^2=u''^2+v''^2$ and $\mathbf{k_1}$ the radial distortion coefficient.

4) Real image coordinate (u_d'',v_d'') to computer frame buffer image coordinate (u_f,v_f) transformation

$$u_f = \mathbf{a_x} \cdot u_d'' + \mathbf{b_x} \cdot v_d'' + \mathbf{c_x} \qquad\qquad v_f = \mathbf{a_y} \cdot u_d'' + \mathbf{b_y} \cdot v_d'' + \mathbf{c_y} \tag{2.4}$$

where $\mathbf{c_x}$ and $\mathbf{c_y}$ represent the image center coordinates (c_u,c_v) and the remaining parameters relate indirectly to the image scale factors (k_x,k_y) and the orthogonality deviation of the image frame buffer referencial axis (θ_1,θ_2) [6].

Assuming the geometry between the image axis and the frame buffer axis presented in fig 1, the transformation between these coordinate systems can be represented by

$$u_f = \frac{k_x \cdot \cos\theta_1}{\cos(\theta_1-\theta_2)} \cdot u_d'' + \frac{k_x \cdot \sin\theta_1}{\cos(\theta_1-\theta_2)} \cdot v_d'' + c_u \qquad v_f = \frac{-k_y \cdot \sin\theta_2}{\cos(\theta_1-\theta_2)} \cdot u_d'' + \frac{k_y \cdot \cos\theta_2}{\cos(\theta_1-\theta_2)} \cdot v_d'' + c_v$$

being

$$\theta_1 = tg^{-1}\frac{b_x}{a_x}, \qquad \theta_2 = -tg^{-1}\frac{a_y}{b_y}, \qquad k_x = \sqrt{\left(a_x^2 + b_x^2\right)}\cdot\cos(\theta_1 - \theta_2), \qquad k_y = \sqrt{\left(a_y^2 + b_y^2\right)}\cdot\cos(\theta_1 - \theta_2).$$

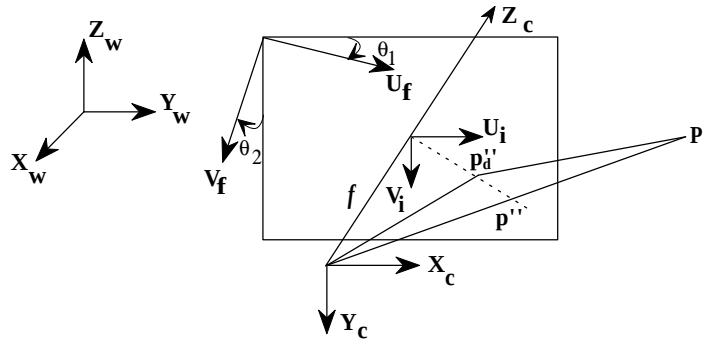

Fig.1 - The camera model

3.Rotation Matrix Calculation

For the rotation matrix calculation we assume the existence of two tridimensional coordinate systems both located at the camera lens center and defined as follows: 1) the world coordinate system $\mathbf{W_r}$ defined orthoghonal and direct; 2) the camera coordinate system $\mathbf{C_r}$ is also defined orthoghonal and direct, and the lens views down the Z axis.

The image plane is located at a distance *f* in front of the lens and is ortoghonal to the optical lens axis. The axis of the image coordinate system $\mathbf{I_r}$ are parallel to the axis of the camera coordinate system $\mathbf{C_r}$.

The rotation matrix defines the transformation between the coordinate systems $\mathbf{W_r}$ and $\mathbf{C_r}$ through the relationship $P_{world} = \mathbf{R}\cdot P_{camera}$, where **R** is an orthoghonal rotation matrix defined as $\mathbf{R} = \mathbf{R}_{(x,\phi)} * \mathbf{R}_{(y,\theta)} * \mathbf{R}_{(z,\psi)}$, resulting

$$\mathbf{R} = \begin{bmatrix} \cos\theta\cos\psi & \cos\theta\sin\psi & -\sin\theta \\ \cos\psi\sin\phi\sin\theta - \cos\phi\sin\psi & \sin\psi\sin\phi\sin\theta - \cos\theta\cos\psi & \sin\phi\cos\theta \\ \cos\psi\sin\theta\cos\phi + \sin\phi\sin\psi & -\sin\phi\cos\psi + \sin\psi\sin\theta\cos\phi & \cos\theta\cos\phi \end{bmatrix} = \begin{bmatrix} r_{11} & r_{12} & r_{13} \\ r_{21} & r_{22} & r_{23} \\ r_{31} & r_{32} & r_{33} \end{bmatrix} \tag{3.1}$$

With respect to the world coordinate system $\mathbf{W_r}$, let (x,y,z) be the coordinates of the image point (u'',v'',*f*) defined in $\mathbf{C_r}$ and obtained from

$$\begin{bmatrix} x & y & z \end{bmatrix}^T = \mathbf{R}\cdot\begin{bmatrix} u'' & v'' & f \end{bmatrix}^T \tag{3.2}$$

Since the lens center is the origin of both coordinate systems, a line passing through the lens and the point (x,y,z) consists of all multiples of (x,y,z). Hence, the line whose perspective projection in the image is (u'',v'') consists of all the points

$$\begin{bmatrix} x_l & y_l & z_l \end{bmatrix}^T \begin{bmatrix} x_l & y_l & z_l \end{bmatrix}^T = \lambda\cdot\begin{bmatrix} x & y & z \end{bmatrix}^T \quad \text{for some constant } \lambda. \tag{3.3}$$

In order to simplify this relationship, we assume that the swing angle ψ over the **Z** axis is zero, so we define without loss of generality the relationship that follows:

$$\begin{bmatrix} x_l \\ y_l \\ z_l \end{bmatrix} \begin{bmatrix} x_l \\ y_l \\ z_l \end{bmatrix} = \lambda\cdot\begin{bmatrix} \cos\theta\cdot u' - f\cdot\sin\theta \\ \sin\theta\cdot\sin\phi\cdot u' + \cos\phi\cdot v' + f\cdot\cos\theta\cdot\sin\phi \\ \cos\phi\cdot\sin\theta\cdot u' - \sin\phi\cdot v' + f\cdot\cos\theta\cdot\cos\phi \end{bmatrix} \tag{3.4}$$

This relationship is valid, since if (u'',v'') is the point on an image whose u_i-v_i plane is rotated by a swing angle ψ, then (u',v') are the coordinates of the corresponding image point whose u_i-v_i plane is rotated by a zero swing angle (ψ=0), and they are related by the relationship

$$\begin{bmatrix} u' \\ v' \end{bmatrix} = \begin{bmatrix} \cos\psi & \sin\psi \\ -\sin\psi & \cos\psi \end{bmatrix} \cdot \begin{bmatrix} u'' \\ v'' \end{bmatrix} \tag{3.5}$$

The basic observation that leads to the rotation matrix calculation, was first presented by Haralick [8] and is based on the fact that there is enough information on the 2D perspective projection of a rectangle's corners to determine the camera look angles. Based on this, let us consider the existence of a rectangle of unknown size located perpendicular to the X_W axis of the $\mathbf{W_r}$ coordinate system (fig.2).

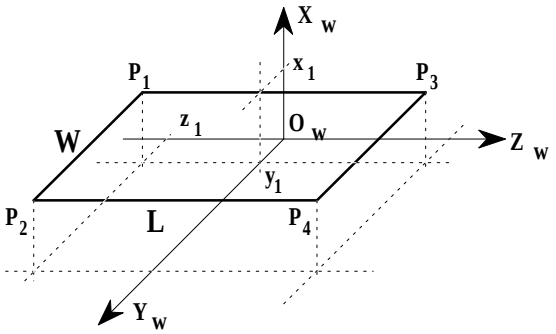

Fig. 2 - Orientation of the rectangle for the rotation matrix calculation

The corners of this rectangle are given by

$$P_1=\begin{bmatrix} x_1 & y_1 & z_1 \end{bmatrix}^T \quad P_2=\begin{bmatrix} x_1 & y_1+W & z_1 \end{bmatrix}^T \quad P_3=\begin{bmatrix} x_1 & y_1 & z_1+L \end{bmatrix}^T \quad P_4=\begin{bmatrix} x_1 & y_1+W & z_1+L \end{bmatrix}^T$$

where $x_1>f$, and the corresponding perspective projection in the image are

$$p_1''=\begin{bmatrix} u_1'' & v_1'' \end{bmatrix}^T \quad p_2''=\begin{bmatrix} u_2'' & v_2'' \end{bmatrix}^T \quad p_3''=\begin{bmatrix} u_3'' & v_3'' \end{bmatrix}^T \quad p_4''=\begin{bmatrix} u_4'' & v_4'' \end{bmatrix}^T .$$

Since the pixels coordinates of these points can only be obtained by means of the image, we need to know in advance the image scale factors and the image center coordinates. We solve this problem assuming some predefined values for these parameters, using the same relationships that Tsai uses in the RAC calibration model [9]. We assume an image center located at the center of the image frame buffer (256, 256), and scale factors given by the relationships $k_x=(S_x\cdot N_{fx})\cdot(d_x\cdot N_{cx})^{-1}$ and $k_y=d_y^{-1}$, where N_{fx} is the number of frame buffer pixels, N_{cx} is the number of CCD sensors in a row, d_x is the distance between CCD sensors in a row, d_y that is the distance between CCD sensors in a column and finally S_x that represents the horizontal uncertainty scale factor. We assume in a first stage an unitary uncertainty scale factor.

Let us begin the calculation of the rotation matrix assuming a swing rotation angle equal to zero ($\psi=0$), which defines the perspective projection points p_i' based on the relationship 3.5. With this assumption, we assume a predefined known swing angle ψ. We also assume a predefined known focal distance *f*.

Using the relationship 3.4 in order to define the four projective lines of the rectangle's corners, we obtain the next matricial equation, which is the basis of this computation.

$$P_i=\lambda_i\cdot\begin{bmatrix} u_i'\cdot\cos\theta-f\cdot\sin\theta \\ u_i'\cdot\sin\theta\cdot\sin\phi+v_i'\cdot\cos\phi+f\cdot\cos\theta\cdot\sin\phi \\ u_i'\cdot\cos\phi\cdot\sin\theta-v_i'\cdot\sin\phi+f\cdot\cos\theta\cdot\cos\phi \end{bmatrix} \text{ with } i=1..4 \tag{3.6}$$

The equations 3.5 and 3.6 are sufficient to obtain the three Euler angles (ψ,θ,ϕ), with all the $\lambda_{i,\ i=1..4}$, and the 3D coordinates of the corners as unknowns.

Through the analysis of these matricial relationships, we observe that the first and third row of equation 3.6 for P_1 and P_2 are identical in order to x_1 and z_1. Conjugating these two equations we establish that

$$f\cdot\sin\theta\cdot\sin\phi\cdot\left(v_2'-v_1'\right)+\cos\theta\cdot\sin\phi\cdot\left(u_2'\cdot v_1'-u_1'\cdot v_2'\right)+f\cdot\cos\phi\cdot\left(u_1'-u_2'\right)=0 \tag{3.7}$$

In an identical manner, the first and third row of equations 3.6 for P_3 and P_4 are identical in order to x_1 and z_1+L, which establishes

$$f\cdot\sin\theta\cdot\sin\phi\cdot\left(v_4'-v_3'\right)+\cos\theta\cdot\sin\phi\cdot\left(u_4'\cdot v_3'-u_3'\cdot v_4'\right)+f\cdot\cos\phi\cdot\left(u_3'-u_4'\right)=0 \tag{3.8}$$

Multiplying 3.7 by (u_3' - u_4') and 3.8 by (u_1' - u_2') and subtracting, results

$$\begin{aligned} f\cdot\sin\theta\cdot\left[\left(v_2'-v_1'\right)\cdot\left(u_3'-u_4'\right)-\left(v_4'-v_3'\right)\cdot\left(u_1'-u_2'\right)\right]= \\ =\cos\theta\cdot\left[\left(u_4'\cdot v_3'-u_3'\cdot v_4'\right)\cdot\left(u_1'-u_2'\right)-\left(u_2'\cdot v_1'-u_1'\cdot v_2'\right)\cdot\left(u_3'-u_4'\right)\right] \end{aligned} \tag{3.9}$$

which by solving for θ yields

$$\theta=\mathrm{tg}^{-1}\frac{\left[\left(u_4'\cdot v_3'-u_3'\cdot v_4'\right)\left(u_1'-u_2'\right)-\left(u_2'\cdot v_1'-u_1'\cdot v_2'\right)\left(u_3'-u_4'\right)\right]}{f\cdot\left[\left(v_2'-v_1'\right)\cdot\left(u_3'-u_4'\right)-\left(v_4'-v_3'\right)\cdot\left(u_1'-u_2'\right)\right]} \tag{3.10}$$

The solution for ϕ is obtained through the same procedure used for θ, multiplying equation 3.7 by (v_4' - v_3') and equation 3.8 by (v_2' - v_1') and subtracting, resulting

$$\phi=\mathrm{tg}^{-1}\frac{f\cdot\left[\left(u_3'-u_4'\right)\cdot\left(v_2'-v_1'\right)-\left(u_1'-u_2'\right)\cdot\left(v_4'-v_3'\right)\right]}{\cos\theta\left[\left(u_2'\cdot v_1'-u_1'\cdot v_2'\right)\left(v_4'-v_3'\right)-\left(u_4'\cdot v_3'-u_3'\cdot v_4'\right)\left(v_2'-v_1'\right)\right]} \tag{3.11}$$

Observing these last two equations, it is apparent that once ψ is known, then ϕ and θ can be solved. The equation that leads to the solution for θ is not unique, since we obtain a new expression based on the fact that the first and second row of equation 3.6 for P_1 and P_3 are similar in order to x_1 and y_1, and the first and second row of equation 3.6 for P_2 and P_4 are similar in order to x_1 and y_1+W. Using the same procedure as before, we obtain an alternate and independent expression for θ, which is

$$\theta=\mathrm{tg}^{-1}\frac{\left[\left(u_2'\cdot v_4'-u_4'\cdot v_2'\right)\cdot\left(u_1'-u_3'\right)-\left(u_1'\cdot v_3'-u_3'\cdot v_1'\right)\cdot\left(u_2'-u_4'\right)\right]}{f\cdot\left[\left(v_1'-v_3'\right)\cdot\left(u_2'-u_4'\right)-\left(v_2'-v_4'\right)\cdot\left(u_1'-u_3'\right)\right]} \tag{3.12}$$

Combining these two expressions for θ we establish the relationship that together with the equation 3.5 defines the expression that allows the calculation of the last Euler angle ψ. Many of the terms included in these equations are ψ rotationally invariant.

Therefore the swing angle ψ is given by

$$\psi=\mathrm{tg}^{-1}\frac{-A\cdot\left(u_1''-u_2''\right)+B\cdot\left(u_3''-u_4''\right)+C\cdot\left(u_1''-u_3''\right)-D\cdot\left(v_2''-v_4''\right)}{A\cdot\left(v_1''-v_2''\right)-B\cdot\left(v_3''-v_4''\right)-C\cdot\left(v_1''-v_3''\right)+D\cdot\left(v_2''-v_4''\right)} \tag{3.13}$$

where

$$A=\frac{u_4''\cdot v_3''-u_3''\cdot v_4''}{E},\ B=\frac{u_2''\cdot v_1''-u_1''\cdot v_2''}{E},\ C=\frac{u_2''\cdot v_4''-u_4''\cdot v_2''}{F},\ D=\frac{u_1''\cdot v_3''-u_3''\cdot v_1''}{F}$$

$$E=f\cdot\left[\left(v_2''-v_1''\right)\left(u_3''-u_4''\right)-\left(v_4''-v_3''\right)\left(u_1''-u_2''\right)\right]\quad F=f\cdot\left[\left(v_1''-v_3''\right)\left(u_2''-u_4''\right)-\left(v_2''-v_4''\right)\left(u_1''-u_3''\right)\right]$$

The values obtained for ψ present an ambiguity of 180 degrees, whereas the values for θ and ϕ present an ambiguity of 90 degrees. Values outside this range for the pan and tilt angles correspond to the camera looking into the hemisphere behind itself.

4. Translation over X and Y and uncertainty scale factor S_x

Until now, we assumed that the two coordinate systems $\mathbf{W_r}$ and $\mathbf{C_r}$ are located at the same origin, and that there is no translation between them. This was not a problem, as the computation of the rotation matrix does not require the knowledge of the coordinates of the rectangle's corners.

Let us now suppose the existence of a translation vector **T** between both coordinate systems. Once the rotation matrix is known, points defined in the coordinate system $\mathbf{W_r}$ can be converted to the camera coordinate system $\mathbf{C_r}$, based on the relationship $P_{camera}=\mathbf{Rot}\cdot P_{world}$ (with $\mathbf{Rot}=\mathbf{R}^{-1}$). From the ratio between the x and y coordinates of a point $P_{(xc,yc,zc)}$ defined in $\mathbf{C_r}$ and its perspective projection u'' and v'' coordinates on the image, we establish the relationship

$$u'' \cdot y_c = v'' \cdot x_c \equiv u''_d \cdot y_c = v''_d \cdot x_c \tag{4.1}$$

Up to now, we have assumed an unitary uncertainty horizontal scale factor, since the rotation matrix calculation was not considerably affected by this assumption. This is not the case for the translation vector. Since we assumed in a first stage a perfect pin-hole camera geometry with a perfectly ortoghonal image and frame buffer coordinate systems, and the relationship 4.1 remains valid even for image points radially distorted, we obtain the following equation

$$S_x \cdot T_x \cdot k_x \cdot (v_f - c_x) - T_y \cdot k_y \cdot (u_f - c_y) + S_x \cdot k_x \cdot (v_f - c_y) \cdot X_{rot} = k_y \cdot (u_f - c_x) \cdot Y_{rot} \tag{4.2}$$

by combining equation 4.1 with the referencial relationship $P_{camera}= R^{-1}\cdot P_{world}$ (with $R^{-1}=R^T$ since R is orthogonal) and the relationships $u_f=S_x\cdot k_x\cdot u''+c_x$, $v_f=k_y\cdot v''+c_y$, being $X_{rot}= r_{11}\cdot x+ r_{21}\cdot y+ r_{31}\cdot z$, and $Y_{rot}= r_{12}\cdot x+ r_{22}\cdot y+ r_{32}\cdot z$.

With the knowledge of the uncertainty scale factor, the value assumed in the beginning for the horizontal scale factor can be updated to be used in the remaining calculations. If this value obtained for S_x is accurate enough, then its value will be one if we obtain new values for the rotation matrix and for T_x, T_y and S_x , using the updated horizontal scale factor. We observed that this conclusion is not valid in the next iteration, but we converge to it after a few iterations.

It is important to make note that the iterative computation of these calibration parameters is performed assuming a perfectly orthogonal image and frame buffer coordinate systems. In order to include the computation of this new parameter, new values for T_x and T_y will be obtained, this time using equations 2.4 combined with equation 4.1, and using the values obtained with the iterative computation for the rotation matrix, T_x, T_y and radial distortion coefficient.

5. Translation over Z, Focal length *f* and Radial distortion coefficient k_1

The basic model that we use in this new methodology for camera calibration follows the one presented by Tsai [9], but with a different focal length calculation. In that model, in order to integrate the radial distortion, it is assumed the existence of two conjugate points, one representing the ideal image point projection while the other point corresponds to the distorted projection point in the image. The relationship between these points is defined in equations 2.3 of the camera model.

Combining equations 2.3 and the perspective projection relationship yields

$$x_c \cdot f + x_c \cdot R_d^2 \cdot f \cdot k_1 - u_d'' \cdot T_z = u_d'' \cdot z_{rot} \qquad y_c \cdot f + y_c \cdot R_d^2 \cdot f \cdot k_1 - v_d'' \cdot T_z = v_d'' \cdot z_{rot} \tag{5.1}$$

being $R_d^2=u_d''^2+v_d''^2$ and $z_{rot}=r_{13}\cdot x+r_{23}\cdot y+r_{33}\cdot z$.

A more detailed study related with these last equations can be found in [9]. Both equations include the effective focal length *f*. However, if we are using a calibration plane that is ortoghonal to the optical axis, the focal length must be considered has a predefined known parameter, since these equations can't find a correct minimum. We solve this problem, using new equations for the calculation of the effective focal length *f*. We obtain in a first stage the translation over Z and the radial distortion coefficient using equations 5.1 assuming a known focal length value, followed by the calculation of the effective focal length of the lens *f*.

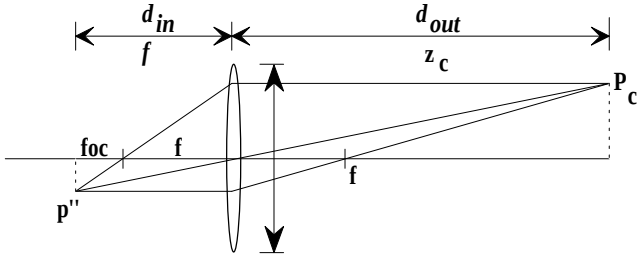

Fig. 3 - The Gauss lens model

We consider the existence of two different focal lengths, being one the effective focal length *f* and the other the lens focal length f obtained through the lens specifications (fig.3). The effective focal length results from the addition of the lens focal length and the focusing distance foc (*f*=f+foc). Combining this observation with the Gauss lens law, we establish the relationship

$$\frac{1}{f}+\frac{1}{z_c}=\frac{1}{f}=\frac{1}{f+foc}+\frac{1}{z_c} \tag{5.4}$$

resulting respectively for the focusing distance foc and for the effective focal length *f* the relationships

$$foc=\frac{f^2}{z_c-f} \qquad f=f+foc=\frac{z_c\cdot f}{z_c-f} \tag{5.5}$$

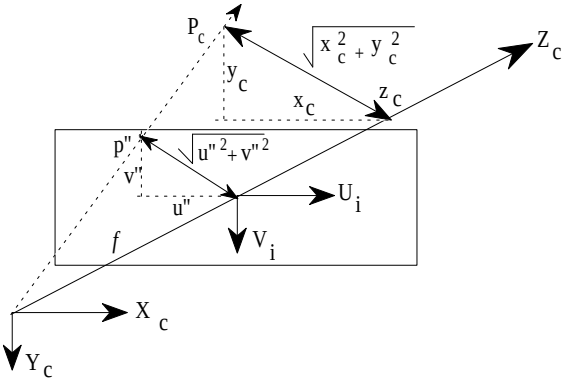

Fig. 4 - Coordinate ratio defined on the plane that includes the line of sight and the optical axis of the camera

In order to obtain a more precise value for the effective focal length, we use this last equation together with the equation that results from the coordinate ratio defined on the plane that includes the line of sight and the optical axis of the lens, as show in figure 4. From this coordinate ratio we obtain the relationship

$$f \cdot \sqrt{x_c^2 + y_c^2} = z_c \cdot \sqrt{u''^2 + v''^2} \tag{5.6}$$

that together with the equation 5.5 defines the equations that we use to obtain the effective focal length *f*.

6. Scale factors, Image center and Orthogonality deviation of the image referencial axis

We have just described a procedure for the calculation of all the extrinsic parameters as well as some of the intrinsic parameters. This set of parameters together with the parameters whose values were assumed characterize the calibration model. However the values of the parameters calculated are affected by errors due to the fact that the values of the intrinsic parameters were assumed at the beginning.

Based on the knowledge of these parameters and using the relationships

$$u_f = \mathbf{a_x} \cdot u_d'' + \mathbf{b_x} \cdot v_d'' + \mathbf{c_x} \qquad v_f = \mathbf{a_y} \cdot u_d'' + \mathbf{b_y} \cdot v_d'' + \mathbf{c_y} \tag{6.1}$$

we can compute a new solution to the intrinsic parameters $\mathbf{a_x}$, $\mathbf{a_y}$, $\mathbf{b_x}$, $\mathbf{b_y}$, $\mathbf{c_x}$ and $\mathbf{c_y}$. The new values calculated for these parameters are much more accurate than the ones initially assumed.

7. Iterative Calibration

Once we have calculated more accurate values for the intrinsic parameters ($\mathbf{a_x}$,$\mathbf{a_y}$,$\mathbf{b_x}$,$\mathbf{b_y}$,$\mathbf{c_x}$,$\mathbf{c_y}$.), more accurate calibration parameters can be expected if they are used in an interactive calibration process. Based on that, we can recalibrate, using now equations 6.1, instead of the relationships of the RAC calibration model.

This iterative procedure is controlled by the accuracy of the image disparity of the projected calibration points. If the mean value of the image disparity converge to a minimum then the iteration is stopped.

8. Accuracy Analysis

In order to obtain high accuracy ground truth for the behaviour of this new camera calibration procedure we simulated the camera calibration setup, taking predefined values for all the calibration parameters and using these values to obtain noise-free homologue 2D-3D test and calibration points. Basically, our goal with these simulated accuracy analyses is to see how much the values obtained for the calibration parameters with the calibration process, miss the predefined values from which the calibration points were obtained. We also analized the behaviour of this new method against to the behaviour of the RAC calibration method, in special, its behaviour with increasing radial distortion and with increasing non-orthogonal image and frame buffer coordinate systems.

The results obtained with these simulated accuracy analysis are presented on graphic I on which we can observe that the accuracy of this new method is considerably better then the accuracy of the RAC method. However, we observed that this new method decreases its performance when the radial distortion increases, while the RAC model doesn't have its performance considerably change. This results from the fact that in this new method we assume in the beginning the existence of non radial distortion. If the radial distortion is considerably large, this assumption affects the initial values of the iterative process in such a manner, that the convergence of the iterative procedure is not so good as in the cases of relatively small radial distortion.

In the RAC method, if the calibration setup presents an orthogonality deviation of the image frame-buffer referencial axis, which results on a calibration points distortion rather than the radial distortion, its performance decreases considerably. This results from the fact that the RAC model doesn't take into account this type of distortion. Yet from the analysis performed with real images, this type of distortion affects the calibration points, and is one of the reasons why the RAC model presents relatively poor accuracy when compared with this new method (graph. II).

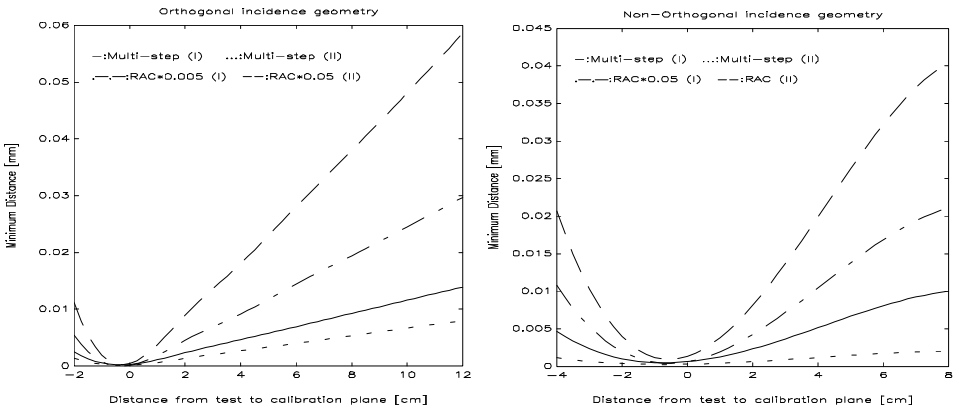

Graph I - Comparative performance analysis between RAC method and Multi-Step method, using simulated images [1];*orthogonal geometry* : f=25mm , *non-orthogonal geometry* : f=16mm
(I):k_1= -0.000567, θ_1-θ_2= -0.0627^o; (II):k_1= -0.000786, θ_1-θ_2= -0.00601^o

The behaviour of these two methods is independent of the focal length, and the angle of incidence only affects the performance of the RAC model. As we can see, the accuracy of the RAC model has better results if the calibration setup presents a non-orthogonal geometry for the optical axis incidence.

Finally, the accuracy of the calibration parameters obtained with this new method is extremely good, but it's slightly affected for situations of considerably large radial distortion. In the case of the RAC model, the accuracy of the calibration parameters changes considerably in the presence of ortoghonality deviation.

In the analysis realized with real images, the performance of this new method was always better than the performance of the RAC calibration model, confirming the results obtained from the simulated analysis. However, we observed that this new method is considerably dependant on the accuracy of the corners coordinates of the rectangle. This dependence results from the fact that the calculation of the rotation matrix is done using only the 2D coordinates of the rectangles corners, and no minimum error computation is used. As a result, care must be taken in the selecction of the rectangle corners, and with the accuracy of the 2D coordinates of the calibration points.

9. Conclusion

A new methodology for robotics camera calibration based on a linear computation and using a coplanar group of calibration points was presented. The main advantage of

[1] One way of measuring the camera calibration accuracy is to see how much the projective line, that is the ray starting from the lens center passing through the image point, misses the correspondent 3D object point. The minimum distance between this projective line and the 3D object point is used as an accuracy camera calibration measurement.

this new method for camera calibration over the RAC method, is that it doesn't require an angle of incidence between the optical axis and the calibration plane over 30 degrees, and the uncertainty factor S_X is calculated during the calibration procedure. This method is based on an *iterative multi-step approach*, and the results obtained through simulated calibrations and real calibrations prove that it is an improvement of the RAC method.

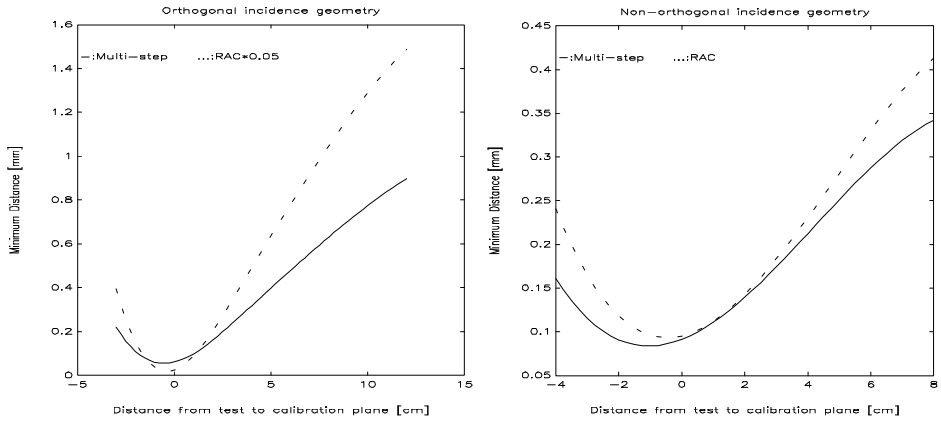

Graph II - Comparative performance analysis between RAC method and Multi-Step method, using real images in the calibration procedure (f=16mm).

10. References

1. H. Martins, J. Birk, R. Kelley, Camera Models Based on Data from Two Calibration Planes, *Computer Graphics and Image Processing*, vol 17, 1981.

2. J. Batista, J. Dias, H. Araújo, A. Traça de Almeida, Monoplanar Camera Calibration for Off-the Shelf TV Camera and Lenses - An Iterative Multi-Spet Approach, *RecPad93-5th Portuguese Conference of Pattern Recognition*, May 13-14, 1993, Porto, Portugal.

3. M. Bowman, A. K. Forrest, Transformation Calibration of a Camera Mounted on a Robot, *Image and Vision Computing*, vol 5, nº4, 1987.

4. M. Penna, Determining Camera Parameters From The Perspective Projection of a Quadrilateral, *Pattern Recognition*, vol 24, nº6, 1991.

5. O. D. Faugeras, G. Toscani, The Calibration Problem for Stereoscopic Vision, *Nato ASI Series*, Vol. F52, 1989.

6. R. Kelley, Calibrage des Cameras Video. Application a l'etude de la derive temporale d'une camera, *Rapport de Recherch* nº 83.006, LAAS, Toulose, 1983.

7. R. Haralick, Using Perspective Transformation in Scene Analysis, *CGIP*, 13, 1980.

8. R. Haralick, Determining Camera Parameters from the Perspective Projection of a Rectangle, *Pattern Recognition*, vol 22, nº3, 1989.

9. R. Y. Tsai, A Versatile Camera Calibration Technique for High-Accuracy 3D Machine Vision Metrology Using Off-the Shelf TV cameras and Lenses, *IEEE Journal of Robotics and Automation*, vol.RA-3, Nº 4, August 1987.

10. R. Y. Tsai, R. K. Lenz, Review of RAC-Based Camera Calibration, *Vision*, vol 5, nº3.

11. T. Echigo, A Camera Calibration Technique using Three Sets of Parallel Lines, *Machine Vision and Applications*, vol 3, pg 159-167, 1990.

12. W. Chen, B. Jiang, 3D Camera Calibration Using Vanishing Points Concept, *Pattern Recognition*, vol 24, nº 1, 1991.